

Electronic Supplementary Information for the manuscript

Surface charge promoting the synthesis of large 2D flat structured graphene–CdS Nanowires–TiO₂ Nanocomposites as versatile visible light photocatalyst

*Siqi Liu, Min-Quan Yang, and Yi-Jun Xu**

State Key Laboratory Breeding Base of Photocatalysis, College of Chemistry and Chemical Engineering, Fuzhou University, Fuzhou, 350002, P. R. China & College of Chemistry and Chemical Engineering, New Campus, Fuzhou University, Fuzhou, 350108, P. R. China

**To whom correspondence should be addressed. Tel. /Fax: +86 591 83779326*

E-mail: yjxu@fzu.edu.cn

Experimental.

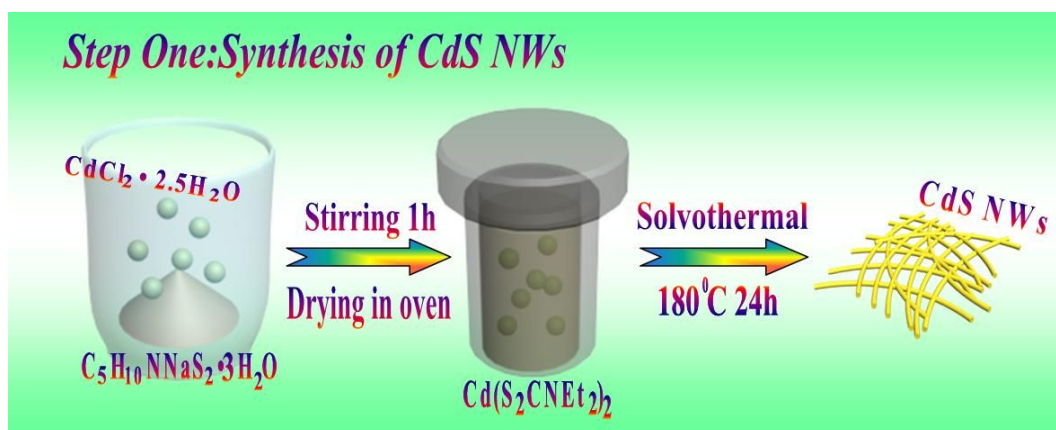
1. Synthesis of CdS nanowires.

Uniform CdS NWs were grown through a modified method,^{S1} as outlined in scheme S1. In a typical process, 1.124 g of cadmium diethyldithiocarbamate (Cd(S₂CNEt₂)₂), prepared by precipitation from a stoichiometric mixture of sodium diethyldithiocarbamate trihydrate and cadmium chloride in deionized water, was added to a Teflon-lined stainless steel autoclave with a capacity of 50 mL. Then, the autoclave was filled with 40 mL of ethylenediamine to about 80% of the total volume. The autoclave was maintained at 180 °C for 24 h and then allowed to cool to room temperature. A yellowish precipitate was collected and washed with absolute ethanol and deionized water to remove residue of organic solvents. The final products were dried in oven at 60 °C for 12 h.

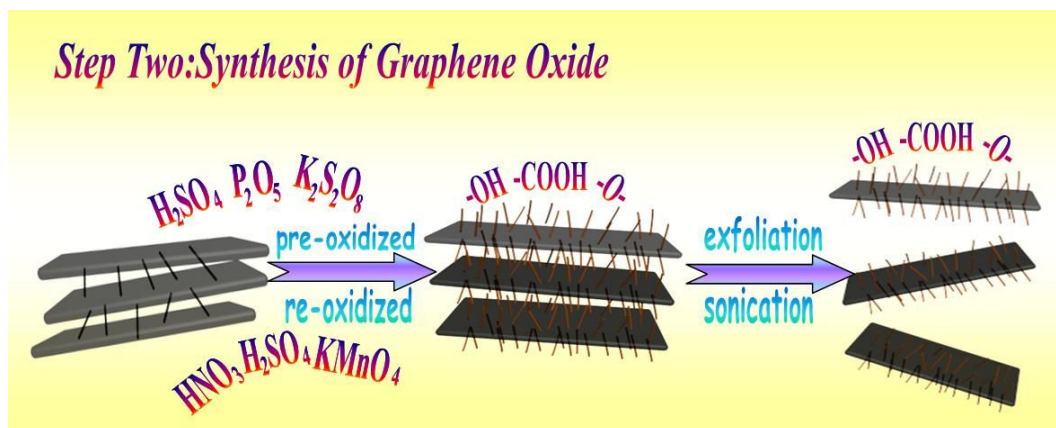
2. Synthesis of Graphene Oxide (GO)

GO was synthesized from natural graphite powder by a modified Hummers method.^{S2-S5} In detail, 2 g of graphite powder (supplied from Sinopharm Chemical Reagent Co., Ltd., China) was put in to a mixture of 12 mL of concentrated H₂SO₄, 2.5 g of K₂S₂O₈, and 2.5 g of P₂O₅. The solution was heated to 80 °C in an oil-bath kept stirring for 24 h. The mixture was then carefully diluted with 500 mL of deionized (DI) water, filtered, and washed until the pH of rinse water became neutral. The product was dried under ambient condition overnight. This pre-oxidized graphite was then subjected to oxidation described as follows. In a typical procedure, pre-oxidized graphite powder was added to a mixture of 120 mL of concentrated H₂SO₄ and 30 mL HNO₃ under vigorous stirring, and the solution was cold to 0 °C. Then, 15 g of KMnO₄ was added gradually under stirring and the temperature of the mixture was kept to be below 20 °C by cooling. Successively, the mixture was stirred at room temperature for 96 h, and then diluted with 1 L of DI water in an ice bath to keep the temperature below 50 °C for 2 h. Shortly after the further diluted with 1 L of DI water, 20 mL of 30% H₂O₂ was then added to the mixture and a brilliant yellow product was formed along with bubbling. The mixture was filtered and washed with 1:10 HCl aqueous solution to remove metal ions

followed by DI water to remove the acid. The filter cake was then dispersed in water by a mechanical agitation. Low-speed centrifugation was done at 1000 rpm for 2 min. The supernatant then underwent two more high-speed centrifugation steps at 8000 rpm for 15 min to remove small GO pieces and water-soluble byproduct. The final sediment was redispersed in water with mechanical agitation or mild sonication using a table-top ultrasonic cleaner, giving a solution of exfoliated GO. The GO separated in the form of a dry, brown powder.



Scheme S1 Schematic flowchart for synthesis of CdS NWs.



Scheme S2 The overall sketch for preparation of graphene oxide (GO).



Fig. S1 Photograph of the experimental setup for photocatalytic reduction of nitroaromatic compounds.



Fig. S2 Photograph of the experimental setup for photocatalytic reduction of Cr (VI).



Fig. S3 Photograph of the experimental setup for photocatalytic oxidation of alcohols into corresponding aldehydes.

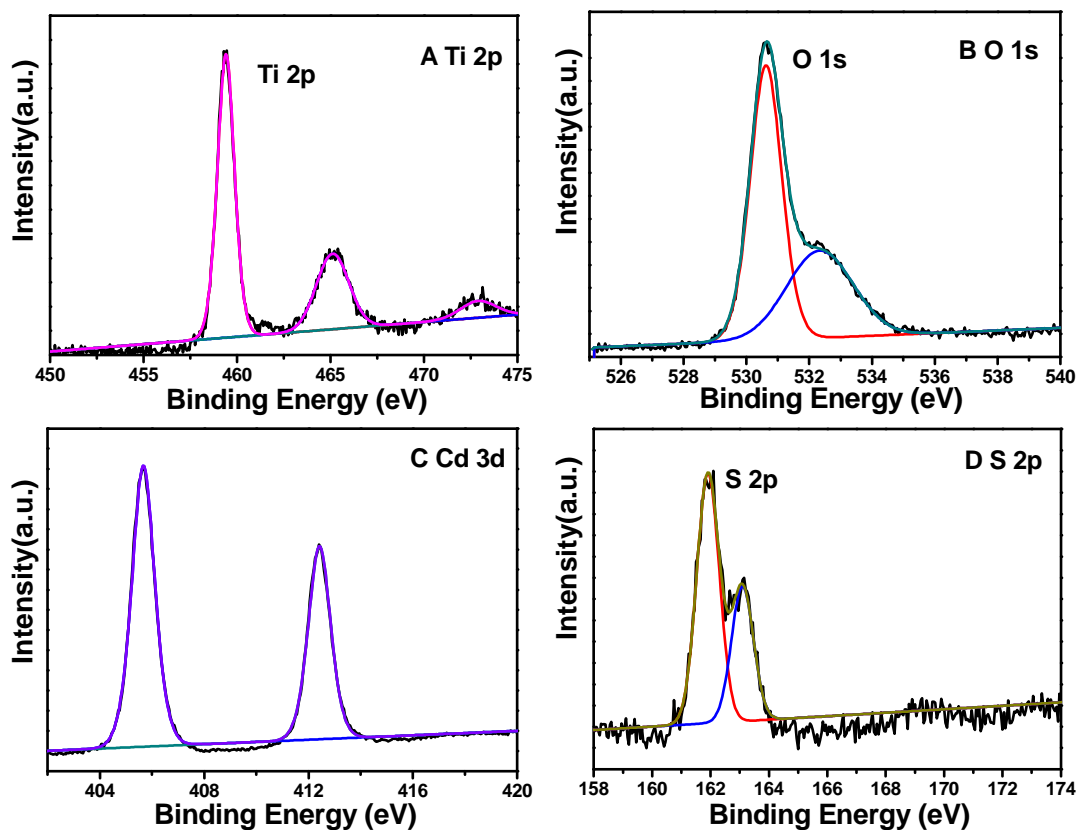


Fig. S4 High-resolution XPS spectrum of Ti 2p region (A), O 1s region (B), Cd 3d region (C) and S 2p region (D).

Note: Obvious photoelectron peaks of Ti, O, Cd and S elements are observed in the XPS survey spectra for the surface of CTG. It can be seen from **Fig. S4A** that two typical peaks of Ti 2p peak located at approximately 459.2 and 464.8 eV correspond to the Ti 2p_{3/2} and Ti 2p_{1/2} binding energies,^{S6-S8} respectively. The O 1s peak in **Fig. S4B** can be further divided into two different peaks with binding energy at ca. 530.7 and 532.2 eV, which can be respectively attributed to the Ti–O in TiO₂ and hydroxyl groups chemisorbed on the surface of the sample.^{S7, S8} As shown in **Fig. S4C**, the spectra of Cd 3d show that the binding energies of Cd 3d_{5/2} and Cd 3d_{3/2} are 405.5 eV and 412.2 eV, respectively.^{S6} The S 2p spectrum, as shown in **Fig. S4D**, consists of two individual peaks S 2p_{3/2} and S 2p_{1/2} with respective binding energies 161.6 eV and 162.8 eV, indicating that the valence state of element S is -2.^{S9, S10}

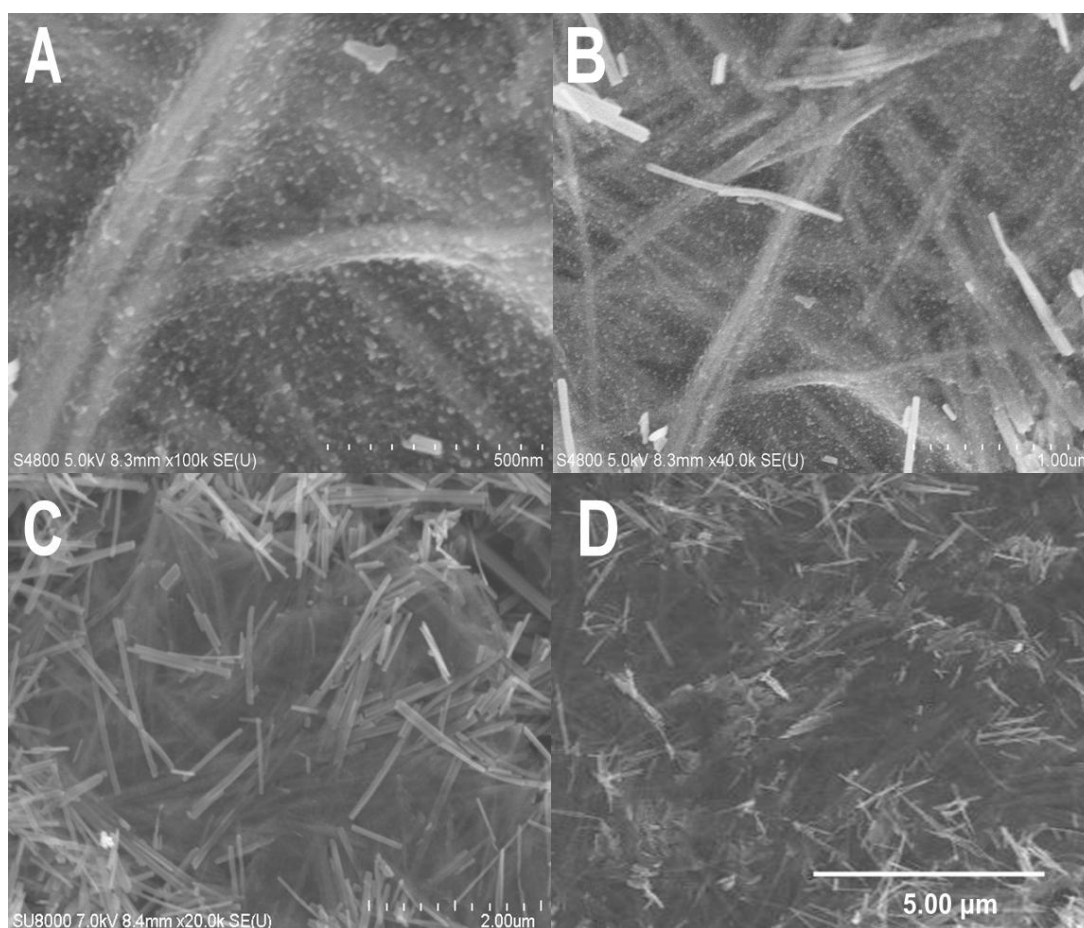


Fig. S5 Typical SEM images of CTG at different magnifications.



Fig. S6 Photographs of the samples of CdS NWs (A), CG (B) and CTG (C).

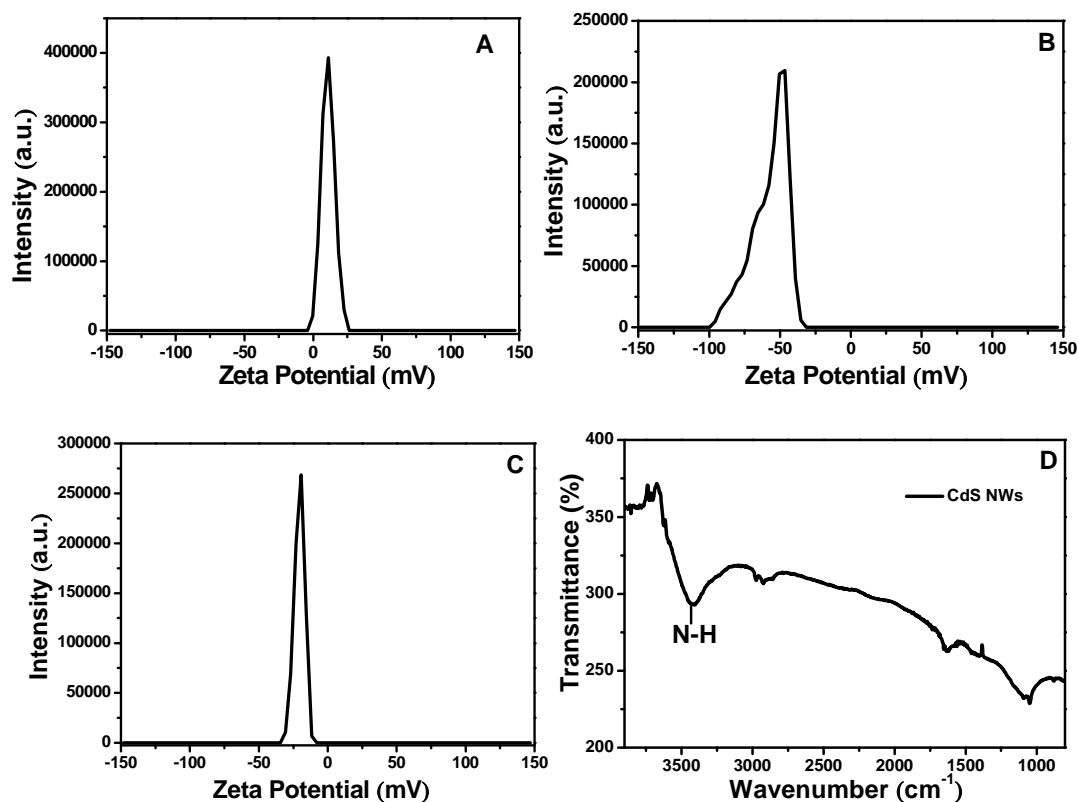


Fig. S7 The zeta potentials (ξ) of CdS NWs (A), GO colloid (B) and TiO₂ nanoparticles (C) in deionized water without adjusting pH values; The Fourier transformed infrared spectra (FT-IR) of CdS NWs at different range of wavenumber (D).

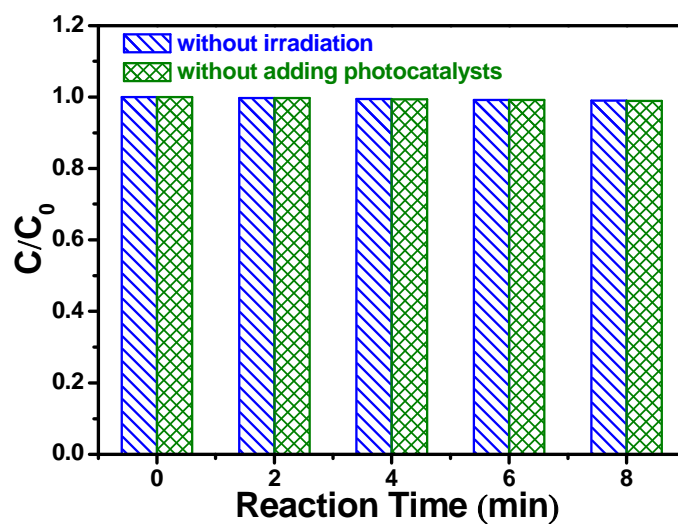


Fig. S8 Blank experiments for reduction of 4-nitroaniline and Cr (VI) without irradiation or without adding photocatalysts.

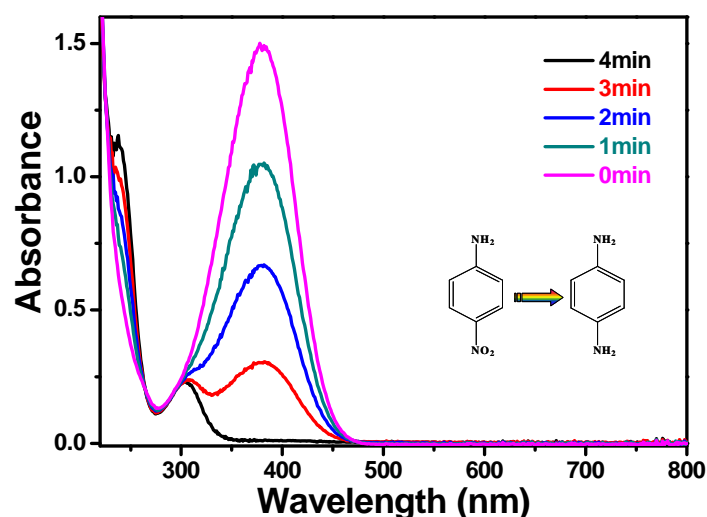


Fig. S9 UV–vis absorption spectra of 4-nitroaniline over the CTG under visible light irradiation with the addition of ammonium formate as quencher for photogenerated holes and N₂ purge under ambient conditions, *i.e.* room temperature and atmospheric pressure taken at regular time interval in the aqueous phase.

Note: The absorption at 380 nm decreases and absorption at 240 nm and 300 nm increases concomitantly, which can be ascribed to the reduction of 4-NA and the formation of 4-phenylenediamine (4-PDA), respectively.^{S11} No other absorption changes demonstrate that there are only two principal species, 4-NA and 4-PDA. According to the ultraviolet–visible light adsorption spectra, before visible light irradiation, there is only one absorption peak at about 380 nm, which is corresponding to the 4-NA. At the end of the reaction at 4 min, the 380 nm peak is disappeared and two new peaks at about 300 nm and 240 nm are achieved, which are corresponding to the 4-PDA, indicates the successful conversion of this selective reduction reaction.

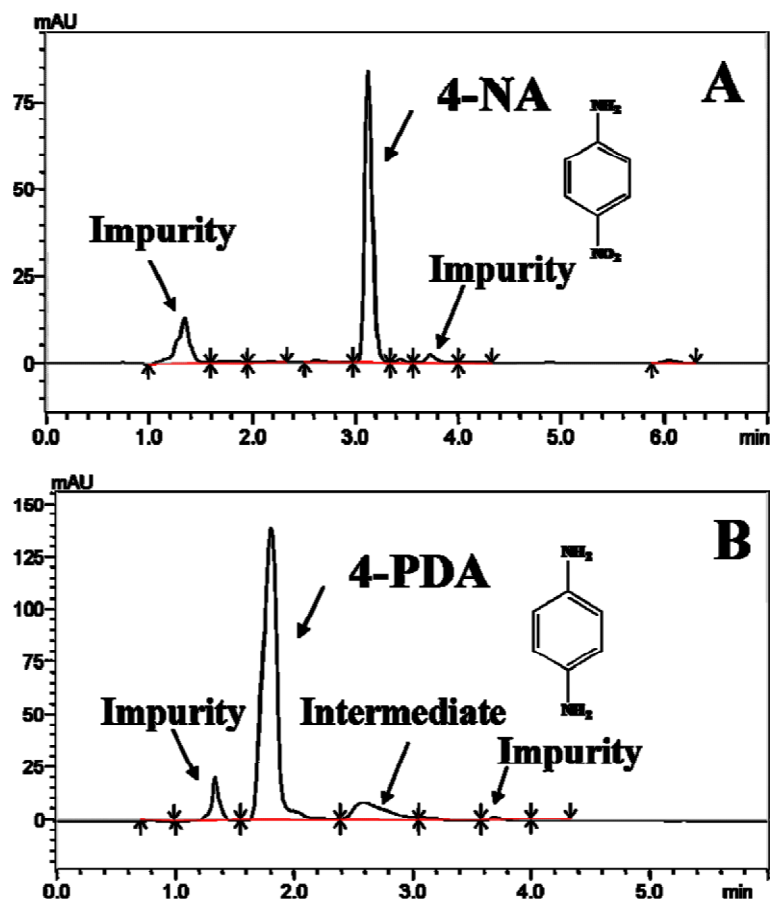


Fig. S10 HPLC analysis (performed on a Shimadzu High Performance Liquid Chromatograph, *i.e.* HPLC–LC20AT which equipped with a C18 column and SPD-M20A photo diode array detector) images of 4-nitroaniline in the aqueous phase under visible light irradiation with the addition of ammonium formate as quencher for photogenerated holes and N₂ purge under ambient conditions, which is taken at regular time interval over the CTG at different reaction time; 0 min for (A) and 4 min for (B).

Note: Analogous results are also observed in the high performance liquid chromatograph (HPLC) spectra by analyzing 0 min and 4 min visible irradiation of the samples. However, due to the purity of the reagents, it is inevitable to observe some minor impurity peaks. In addition, a very minor peak is also observed in the HPLC spectra, which could be ascribed to intermediate products. However, it is clear to see that the impurity and intermediate peaks are very weak, which thus suggests that the very high selectivity is achieved for photocatalytic reduction of nitroaromatic compounds to amino organics.

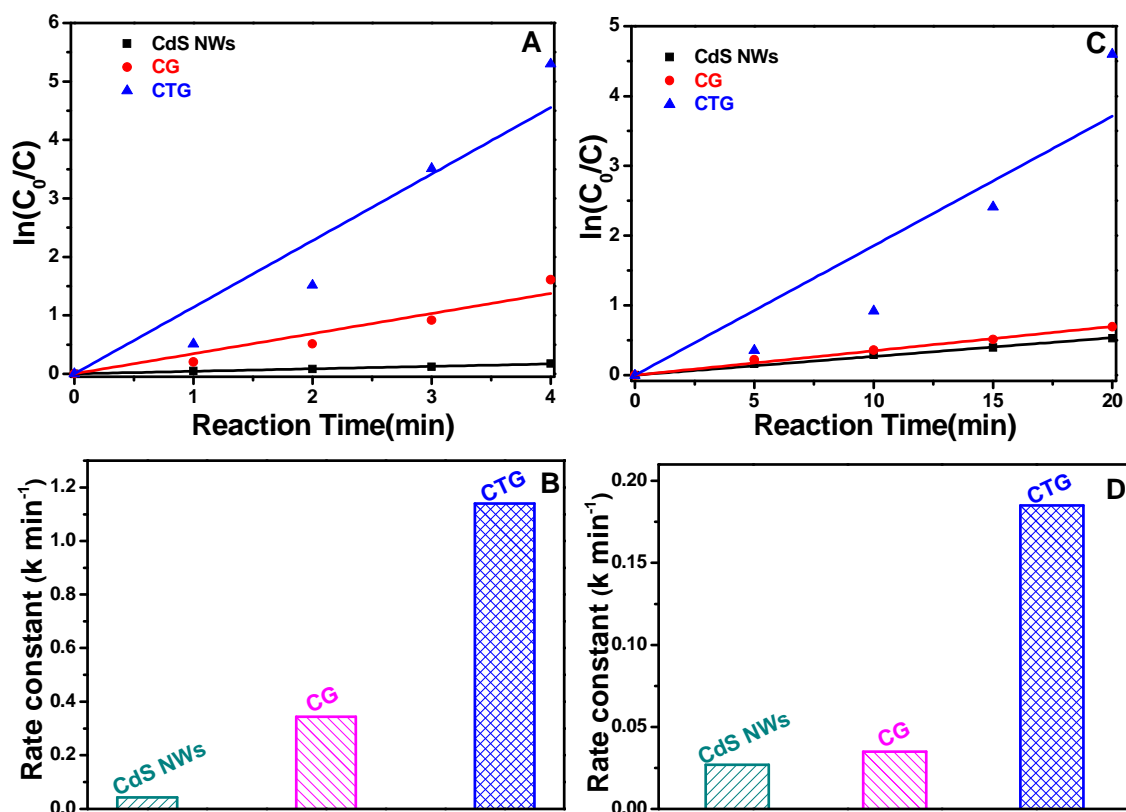


Fig. S11 $\ln(C_0/C)$ versus irradiation time for CdS NWs, CG and CTG for selective reduction of 4-nitroaniline (A), and Cr (VI) (C) the comparison of rate constants over these nanocomposites (B) and Cr (VI) (D).

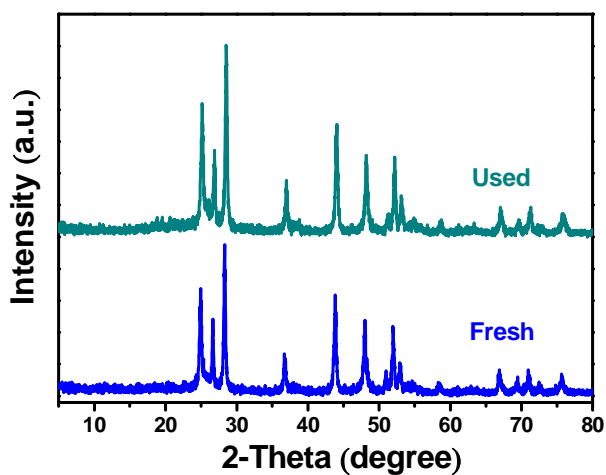


Fig. S12 XRD patterns of the CTG before and after photo-reaction.

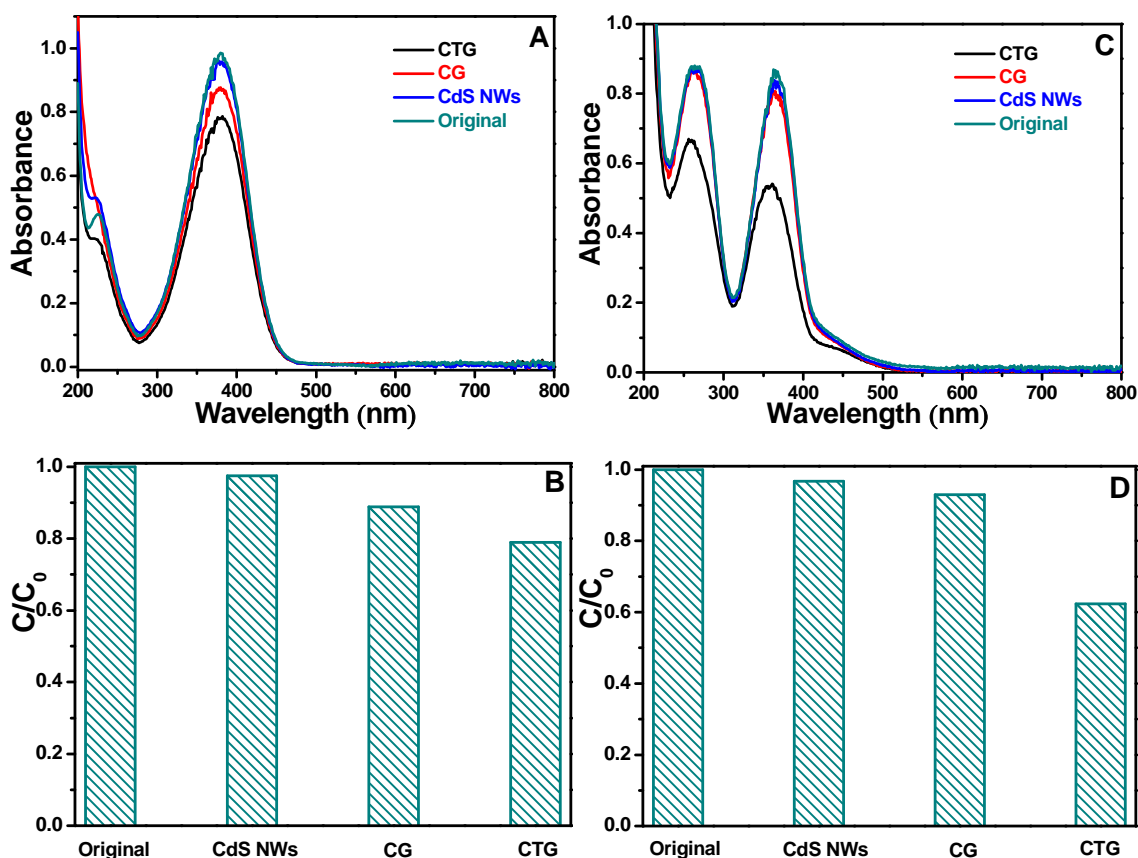


Fig. S13 UV-vis absorption spectra of 4-nitroaniline and Cr (VI) over CdS NWs, CG and CTG under adsorption equilibrium (A and C, respectively) and column plot showing the remaining 4-nitroaniline and Cr (VI) in solution after being kept in the dark for 2 h until adsorption equilibrium of the 4-nitroaniline solution (B and D, respectively).

Note: 10 mg of the samples were added into 20 mL of 4-NA ($10 \text{ mg}\cdot\text{L}^{-1}$) and 20ml of Cr (VI) ($20 \text{ mg}\cdot\text{L}^{-1}$) in a quartz vial. The adsorption equilibrium of the 4-NA and Cr (VI) was achieved after being kept in the dark for 2 h.

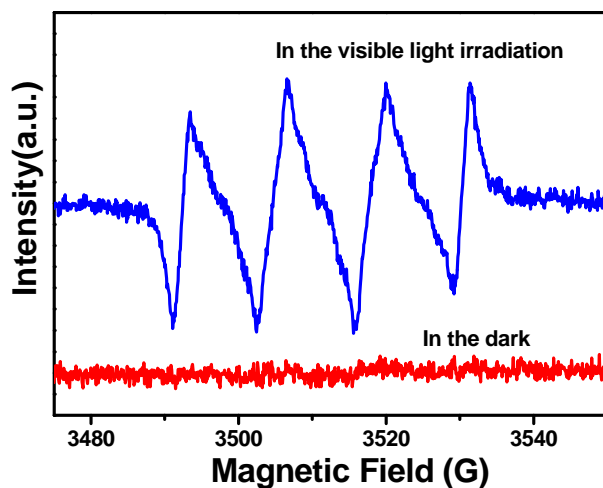


Fig. S14 ESR spectra of superoxide radical species trapped by DMPO over the CTG suspension in the BTF solution without or with visible light irradiation ($\lambda > 420 \text{ nm}$); no hydroxyl radicals are detected.

Table S1 Summary of surface area, pore volume and pore size of the as-prepared CdS NWs, CG and CTG for comparison.

| Samples | S_{BET} (m^2/g) ^a | Total pore volume (cm^3/g) ^b | Average pore size (nm) ^c |
|---------|---|---|-------------------------------------|
| CdS NWs | 12 | 0.09 | 31 |
| CG | 29 | 0.11 | 15 |
| CTG | 121 | 0.21 | 7 |

^a BET surface area is calculated from the linear part of the BET plot.

^b Single point total pore volume of the pores at $P/P_0 = 0.99$.

^c Adsorption average pore width ($4V/A$ by BET).

References

- (S1) L. Wang, H. Wei, Y. Fan, X. Gu and J. Zhan, *J. Phys. Chem. C*, 2009, **113**, 14119.
(S2) W. S. Hummers and R. E. Offeman, *J. Am. Chem. Soc.*, 1958, **80**, 1339.
(S3) L. J. Cote, F. Kim and J. Huang, *J. Am. Chem. Soc.*, 2008, **131**, 1043.
(S4) N. I. Kovtyukhova, P. J. Ollivier, B. R. Martin, T. E. Mallouk, S. A. Chizhik, E. V. Buzaneva and A. D. Gorchinskiy, *Chem. Mater.*, 1999, **11**, 771.
(S5) D. Pan, S. Wang, B. Zhao, M. Wu, H. Zhang, Y. Wang and Z. Jiao, *Chem. Mater.*, 2009, **21**, 3136.
(S6) L. Wu, J. C. Yu and X. Fu, *J. Mol. Catal. A: Chem.*, 2006, **244**, 25.
(S7) J. C. Yu, J. Yu, H. Y. Tang and L. Zhang, *J. Mater. Chem.*, 2002, **12**, 81.
(S8) J. C. Yu, J. Yu and J. Zhao, *Appl. Catal., B*, 2002, **36**, 31.
(S9) S. Rengaraj, S. Venkataraj, S. H. Jee, Y. Kim, C.-w. Tai, E. Repo, A. Koistinen, A. Ferancova and M. Sillanpää, *Langmuir*, 2010, **27**, 352.
(S10) N. Zhang, S. Liu, X. Fu and Y.-J. Xu, *J. Mater. Chem.*, 2012, **22**, 5042.
(S11) C.-Y. Chiu, P.-J. Chung, K.-U. Lao, C.-W. Liao and M. H. Huang, *J. Phys. Chem. C*, 2012, **116**, 23757.